Geophysical Research Letters

RESEARCH LETTER
10.1029/2023GL105850

The Impact of Rotation on Tropical Climate, the Hydrologic Cycle, and Climate Sensitivity

Levi G. Silvers[1,2], **Alyssa M. Stansfield**[2], **and Kevin A. Reed**[1]

[1]School of Marine and Atmospheric Sciences, State University of New York at Stony Brook, Stony Brook, NY, USA, [2]Department of Atmospheric Science, Colorado State University, Fort Collins, CO, USA

Key Points:

- Rotation leads to a decreased intensity of the overturning circulation but increased mean precipitation and precipitable water
- Static stability increases with rotation, net radiative cooling remains approximately constant, resulting in a smaller subsidence velocity
- Rotating experiments have a larger effective climate sensitivity relative to RCE experiments mostly due to longwave radiative changes

Supporting Information:

Supporting Information may be found in the online version of this article.

Correspondence to:

L. G. Silvers,
levi.silvers@colostate.edu

Citation:

Silvers, L. G., Stansfield, A. M., & Reed, K. A. (2024). The impact of rotation on tropical climate, the hydrologic cycle, and climate sensitivity. *Geophysical Research Letters*, *51*, e2023GL105850. https://doi.org/10.1029/2023GL105850

Received 11 DEC 2023
Accepted 14 FEB 2024

Abstract This work explores the impact of rotation on tropical convection and climate. As our starting point, we use the RCEMIP experiments as control simulations and run additional simulations with rotation. Compared to radiative convective equilibrium (RCE) experiments, rotating RCE (RRCE) experiments have a more stable and humid atmosphere with higher precipitation rates. The intensity of the overturning circulation decreases, water vapor is cycled through the troposphere at a slower rate, the subsidence fraction decreases, and the climate sensitivity increases. Several of these changes can be attributed to an increased flux of latent and sensible heat that results from an increase of near-surface wind speed with rotation shortly after model initialization. The increased climate sensitivity results from changes of both the longwave cloud radiative effect and the longwave clear-sky radiative fluxes. This work demonstrates the sensitivity of atmospheric humidity and surface fluxes of moisture and temperature to rotation.

Plain Language Summary Many useful studies of the tropical regions of Earth have neglected to include rotation; however, phenomena such as tropical cyclones and atmospheric waves are fundamentally tied to rotation. This work compares models of the tropics with and without rotation. Compared to experiments without rotation, rotating experiments have a more humid and stable atmosphere. Although water vapor is cycled through the atmosphere at a slower rate, the precipitation rate increases. The climate sensitivity also increases due to changes in both clouds and water vapor. Many of these changes are the result of increased wind speeds. We argue that idealized modeling of Earth's tropical regions should include not just stationary experiments but also experiments that include rotation.

1. Introduction

The hydrologic cycle on Earth is of the utmost importance to both the daily weather cycle and the global energy balance that determines the climate (O'Gorman et al., 2012; Webster, 1994). Part of the fascinating complexity of the hydrologic cycle derives from the different roles that water condensate and vapor play in the flow of energy through the climate system; however, the ease with which water transitions between phases challenges the prediction of future atmospheric states. While condensate is closely tied to energetic constraints of surface evaporation and net atmospheric radiative cooling, vapor amount is constrained by the Clausius-Clapeyron (CC) relation. The CC relation describes how the saturation vapor pressure depends on temperature, but it does not determine how close to saturation the atmosphere will be. Extreme changes in the degree of saturation of the atmosphere can lead to drastic changes of climate including either a runaway warming scenario (more saturated) or a snow and ice covered planet (less saturated; Pierrehumbert et al., 2007). The spatial structure of the humidity and clouds can also influence the hydrologic cycle and the mean energetics (Pierrehumbert, 1995) of the climate system. For example, the horizontal structure of convective systems influences the domain mean humidity and the radiant flux of energy (Bretherton et al., 2005; Muller & Held, 2012; Tobin et al., 2012; Wing & Emanuel, 2014). On Earth, the dominant influence of rotation on the horizontal distribution of the clouds and water vapor is apparent in numerous phenomena including tropical cyclones, the Madden-Julian Oscillation (MJO), convectively coupled waves, and the Intertropical Convergence Zone (ITCZ). These modes of oscillation and variability play a major role in the organization of tropical precipitation on Earth (e.g., Kiladis et al., 2009). Part of the motivation for this study is a desire to better understand how rotation influences and modifies the balance between radiation, convection, and water vapor in the tropical regions of earth.

Multiple important characteristics of the tropical atmosphere are realistically captured by simulations of radiative convective equilibrium (RCE) (e.g., Bony et al., 2016), and previous studies have shown that useful similarities

exist between the basic state (e.g., cloud profiles) of RCE simulations and the deep tropics of the parent general circulation models (GCMs) (Popke et al., 2013; Reed et al., 2021). For example, the stability iris mechanism (Bony et al., 2016) is robustly represented in models of RCE, Earth system models, and observations. The stability iris mechanism is the process whereby warmer cloud base temperatures lead to rising cloud tops that maintain an approximately constant temperature (Hartmann & Larson, 2002) but encounter a larger static stability, with the result of less detrainment and a smaller anvil cloud fraction. In contrast to RCE, the rotation of Earth facilitates the organization of tropical convection into aggregated systems which play a substantial role in the tropical energy budget, the atmospheric static stability, and the MJO (Arnold & Randall, 2015; Bony et al., 2016; Wing et al., 2017). The ubiquity of rotating storm systems on Earth and the persistent surface temperature gradients imply that while RCE has successfully guided fundamental advances in our understanding of the Earth's climate (e.g., Manabe & Wetherald, 1967), it is likely that rotation plays an important role in setting some of the basic characteristics of Earth's tropical regions.

Tropical cyclones and tropical cyclone-like vortices (TCLVs) have been simulated in RCE-like states with a variety of configurations including cloud resolving models (CRMs) that use a fixed rotation rate in limited area domains (Carstens & Wing, 2022; Cronin & Chavas, 2019; Held & Zhao, 2008; Khairoutdinov & Emanuel, 2013; Wing et al., 2016), global simulations using a fixed rotation rate (Reed & Chavas, 2015), and global simulations that have a more realistic latitude-dependent rotation rate (Arnold & Randall, 2015; Chavas & Reed, 2019; Kirtman & Schneider, 2000; Merlis et al., 2016; Stansfield & Reed, 2021). Most of these previous studies focused on the resulting TCLVs (Held & Zhao, 2008; Reed & Chavas, 2015; Shi & Bretherton, 2014; Stansfield & Reed, 2021) or specific tropical phenomena such as the MJO (Arnold & Randall, 2015) rather than a comparison between the RCE and RRCE states. These previous studies have yielded many interesting results. For example, Khairoutdinov and Emanuel (2013) showed that f-plane RCE simulations had larger precipitation rates and precipitable water, as well as a decreased deep-convective mass flux. One motivation for the present paper is the desire to consistently compare RCE and RRCE states within the same modeling framework to determine why rotating states seem to have more precipitable water and higher rates of precipitation. This will increase our understanding of how the ubiquitous rotation of Earth influences the hydrologic cycle and how the resulting idealized state influences the climate feedback parameter.

2. Methods and Background

To investigate the impact of rotation on an Earth-like tropical climate, this study uses two global climate models run with full physics parameterizations in an idealized configuration. We use the Community Atmospheric Model 5 and 6 (CAM5 and CAM6, respectively) in a state of either RCE or with rotation added (RRCE). Both of these global models run with a horizontal grid spacing of approximately 1° and have parameterized deep convection. Our RCE simulations adopt the RCEMIP protocols of Wing et al. (2018). The RRCE simulations presented in this paper only differ from the RCE simulations of Wing et al. (2020) and Reed et al. (2021) by the addition of planetary rotation in the form of an Earth-like Coriolis parameter ($f = 2\Omega \sin \phi$, where the angular velocity is $\Omega = 7.292115e^{-5}$ rad s^{-1} and the latitude is given by ϕ). This work provides a link between the RRCE CAM experiments of Stansfield and Reed (2021) and RCE experiments using CAM (Reed et al., 2015, 2021; Silvers, Reed, & Wing, 2023) at conventional climate model resolutions. We analyze simulations with uniform and fixed SSTs of 295, 300, and 305 K, integrated for 2 years with most analysis focused on the last year of the simulations. Further details of the setup, the models, and the parameters for tracking the TCLVs in the RRCE simulations are in Supporting Information S1.

Overall, the CAM5 and CAM6 RCE climates are similar, relative to the range of climates simulated among other models in RCEMIP (Reed et al., 2021; Wing et al., 2020), and the results presented in this paper are robust between both models. However, there are a few important differences. For example, CAM5 has more low-level clouds and substantially more cloud liquid below 700 hPa (Figures S1 and S2 in Supporting Information S1). When analyzing the radiative response at the top of the atmosphere to the increase of SST from 295 to 305 K, CAM6 has a smaller feedback parameter (Reed et al., 2021), implying a correspondingly higher climate sensitivity. This paper primarily presents results in the context of CAM6, with further discussion of the comparison between CAM5 and CAM6 contained in Supporting Information S1.

Table 1
Domain Mean Statistics Averaged Over the Last Year of Experiments From CAM6

Configuration	SST (K)	P (mm/day)	PW (kg/m^2)	CF	OLR (W/m^2)	ASR (W/m^2)	LH (W/m^2)	SH (W/m^2)	V_{rms} (m/s)	SF
CAM6										
RCE	295	2.28	21.41	0.56	245.42	326.08	66.06	11.95	2.25	0.70
RRCE	295	2.80	26.69	0.59	248.62	328.91	80.98	10.41	6.26	0.67
RCE	300	2.93	31.72	0.49	260.68	326.49	84.93	12.60	2.10	0.77
RRCE	300	3.36	41.61	0.76	256.24	326.40	97.15	9.76	6.64	0.70
RCE	305	3.74	51.48	0.96	270.63	324.25	108.32	11.58	2.63	0.76
RRCE	305	3.88	65.18	0.84	260.08	321.19	112.28	8.31	5.40	0.70

Note. Shown is the configuration, the sea surface temperature SST, mean precipitation P, precipitable water PW, cloud fraction CF, outgoing longwave radiation OLR, the absorbed solar radiation at the top of the atmosphere ASR, the latent LH and sensible heat fluxes SH to the atmosphere, the root mean square velocity of the lowest model level V_{rms}, and the subsidence fraction SF.

3. The Impact of Rotation on the Hydrologic Cycle

Adding rotation to RCE alters the hydrologic cycle and its sensitivity to warming. These changes manifest in the mean precipitation, *P*, the surface fluxes of energy, and the distribution of humidity throughout the troposphere. Rotation, as with warming, leads to a substantial increase in the surface flux of latent heat (*LH*), *P*, and precipitable water (*PW*) (Table 1). The rotating atmosphere is more humid, with the *RH* between 200 and 600 hPa being 10%–20% larger than in RCE. This is the case not only in the domain mean values (Figures S1 and S2 in Supporting Information S1) but also for the regional patterns of *RH* (Figure 1, Figure S3 in Supporting Information S1). Non-rotating simulations are characterized by large regions with an *RH* less than 10%. Such regions of very low humidity in the upper troposphere are an important element of the radiative response to warming through their influence on outgoing longwave radiation (Pierrehumbert, 1995).

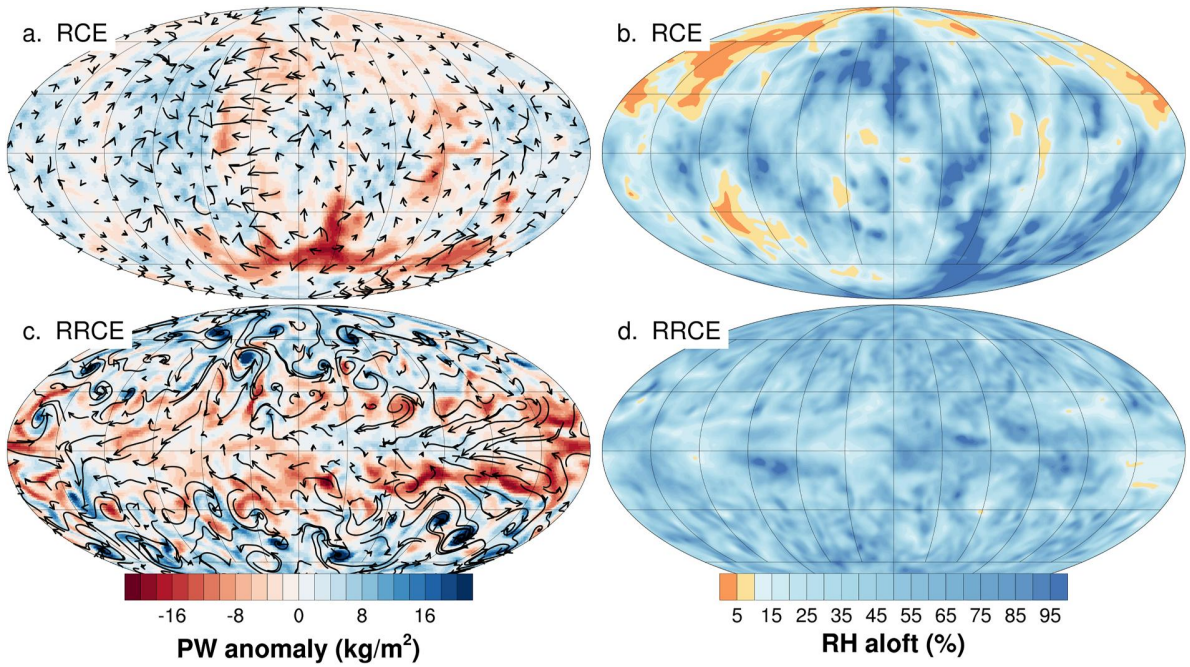

Figure 1. Comparison between RCE (top) and RRCE (bottom) simulations. On the left is shown an hourly averaged snapshot of the precipitable water (*PW*) anomaly and the wind vectors on the lowest model level. On the right is shown the *RH* on the 445 hPa pressure level, averaged over 1 week. Data is from the simulation with a constant SST of 300K at the end of the 2nd year of simulation using the CAM6 model.

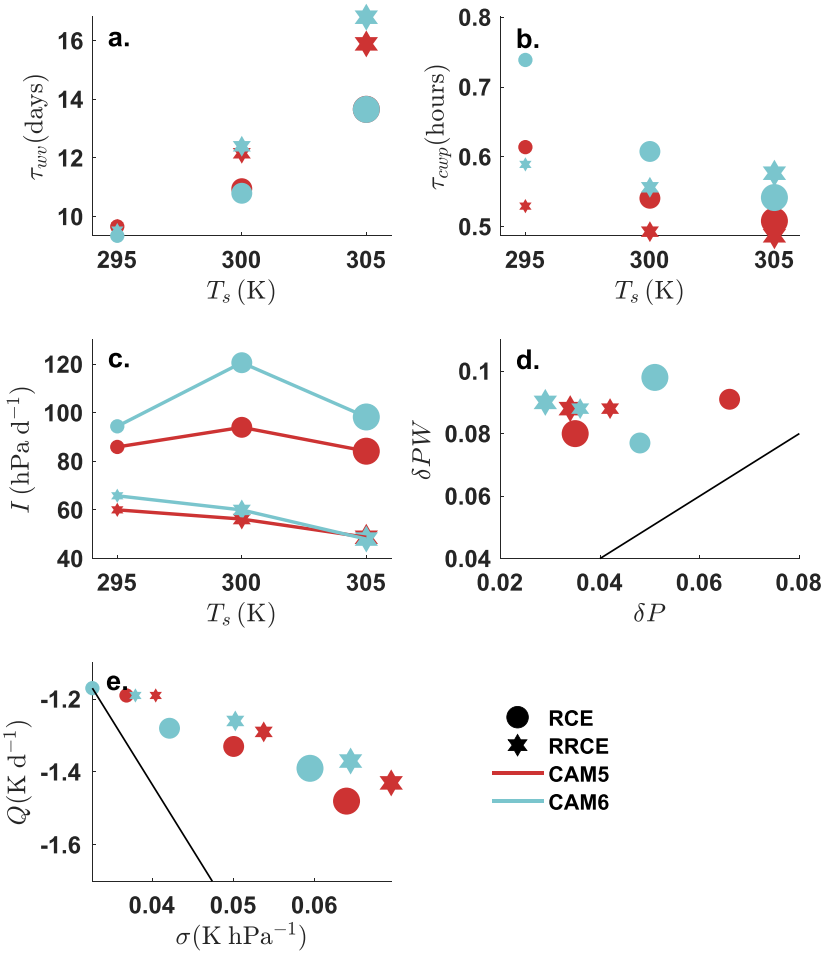

Figure 2. Mean values from RCE (circles) and RRCE (stars) simulations with CAM5 (red) and CAM6 (blue). (a) residence time of integrated water vapor (days), (b) residence time of condensed water (hours), (c) intensity of circulation, computed over 5-day chunks, (d) scatter plot of the differential rate of change of *PW* and *P*, (e) net radiative heating (Q) and static stability (σ), vertically averaged between 800 and 300 hPa. Increasing marker size corresponds to simulations with higher SST. The 1:1 line is shown in black in (d). Example values for a constant ω_d are shown by black line in (e).

Two informative metrics of the hydrologic cycle are the residence times (or inverse cycling rates) of water vapor and condensate, referred to as τ_{wv} and τ_{cwp}, respectively. These are calculated as *PW*/*P* and *CWP*/*P*, where *CWP* is the column integrated liquid and ice condensate. Rotation increases the residence time of water vapor (Figure 2a) and slightly decreases the residence time of condensates (Figure 2b). The increase of τ_{wv} is directly related to the increased humidity, as measured by *PW*. In all experiments with rotation, the *PW*, *P*, and *LH* increase (Table 1). When the simulations are equilibrated, increased *LH* is balanced by increased *P*. Therefore, the increased *LH* shown in Table 1 is not the source of the increased humidity in the RRCE simulations. During the initial adjustment period (about 50 days) of the simulations, several interesting details emerge (Figures S4 and S5 in Supporting Information S1). Almost immediately, the root mean square velocity of the lowest atmospheric model level, V_{rms}, slightly increases and then around days 10–15, V_{rms} increases substantially. During this same period, both *LH* and *SH* increase, presumably due to the influence of larger V_{rms}. As the flux of moisture and sensible heat increase, the temperature of the lowest atmospheric level and *PW* increase. *P* also increases during the adjustment period, but not by as much as the *LH* (Figure S5 in Supporting Information S1). After about 3–4 weeks, *LH* and *P* have reached a balance that is then maintained for the rest of the simulations, but only after a period of time when the flux of moisture into the atmosphere by *LH* was greater than the flux of moisture out of the atmosphere by *P* (Figure S4 in Supporting Information S1). *SH* and the low-level temperature cannot both increase indefinitely because *SH* is directly proportional to the gradient of temperature from the surface to the lower atmosphere. As the temperature of the lowest atmospheric level increases and approaches the value of the SST, the *SH* will decrease, as reflected in

Table 1. We conclude that both the increased humidity and the increased temperature of the RRCE simulations compared to RCE are the result of the adjustment to larger values of V_{rms} during the first few weeks of simulation.

Multiple pieces of evidence indicate that the overturning circulation decreases in magnitude when rotation is included. This is distinct from the numerous studies that have shown (e.g., Bony et al., 2013; Held & Soden, 2006; Knutson & Manabe, 1995) that the tropical overturning circulation decreases with warming. The dynamically driven intensity of the large-scale circulation, I (hPa d^{-1}) is calculated as $I = \omega^{\downarrow} - \omega^{\uparrow}$ and approximates the strength of the overturning circulation. I provides a joint measure of the ascending and descending regions, where $\omega^{\uparrow}$ (hPa d^{-1}) and $\omega^{\downarrow}$ (hPa d^{-1}) are the mean 500 hPa pressure velocities in ascending and descending regions, respectively (Bony et al., 2013). Our results show a fairly large decrease of I (30–40 hPa d^{-1}) when rotation is added (Figure 2c). Another measure of the overturning circulation, the mass flux from the boundary layer, also decreases as a result of rotation (Figure 2d). Following the arguments of Betts (1998) and Held and Soden (2006), an approximation of the mass exchange between the boundary layer and the free troposphere can be inferred from the rates of change of P and PW (δP and δPW; detail in Supporting Information S1). The larger rate of change in PW relative to P (Figure 2d) implies that the precipitating convective mass flux from the boundary layer must be decreasing. This decrease with rotation is indicated by the shift further from the 1:1 line of the RRCE (stars) relative to the RCE (circles) simulations in Figure 2d. Based on fundamental properties of the tropics, $\omega^{\downarrow}$ is constrained to be approximately equal to the diabatically driven subsidence velocity, $\omega_d = -Q/\sigma$, where Q (K d^{-1}) is the net atmospheric radiative heating and σ (K hPa^{-1}) is the static stability (see Supporting Information S1 for details). No such constraint is present for $\omega^{\uparrow}$ which is driven by the regions of deep convective activity. While $\omega^{\downarrow}$ does decrease in magnitude with rotation, the change of I is largely driven by the decreasing magnitude of $\omega^{\uparrow}$ (Table S3 in Supporting Information S1), consistent with findings from the RCEMIP warming simulations (Silvers, Reed, & Wing, 2023).

4. Atmospheric Stability, Clouds, and the Climate Sensitivity

Closely connected to $\omega^{\downarrow}$, $\omega^{\uparrow}$, and the amount of anvil clouds that are driven by convective outflow is the atmospheric static stability, σ. As the surface warms, σ increases and Q often intensifies (e.g., Bony et al., 2016; Zelinka & Hartmann, 2010). We find an additional increase of σ when rotation is included (Figure 2e). This is likely due to the warmer troposphere in the RRCE cases that results from the initial increase of SH discussed in the previous section (see Figures S5, S10, and S11 in Supporting Information S1), which can enhance convective mixing and thereby increase σ (Tomassini et al., 2014). We also find a warmer cloud base temperature in the RRCE cases (Figure S12 in Supporting Information S1), which implies an increased σ at the level of convective outflow (Bony et al., 2016). Increased σ then tends to dampen convective activity and leads to a decreased magnitude of both $\omega^{\uparrow}$ and $\omega^{\downarrow}$. We find that although σ increases with rotation, Q changes little. This results in a decrease of ω_d in RRCE relative to RCE (Figure 2e). Consistent with previous studies, ω_d also decreases with warming for all simulations.

The global mean cloud fraction increases with rotation in 4 out of 6 simulations (Table 1, and Table S1 in Supporting Information S1). Clouds, as diagnosed by liquid and ice condensate, show some systematic differences when viewed as vertical profiles. Simulations with rotation have more low-level clouds (when present), fewer clouds between 350 and 800 hPa, and more upper level clouds (Figures S1, S2, S6, S7, and S12 in Supporting Information S1). Moisture, clouds, and precipitation for CAM5 and CAM6 in RCE were shown to organize from homogeneous initial conditions into aggregated structures (Reed et al., 2021). Carstens and Wing (2022) and Carstens and Wing (2023) showed a large range of aggregated states that result from a latitude-dependent Coriolis parameter in cloud resolving simulations. In our RRCE cases, despite the presence of TCLVs (see Section 5), aggregation, as measured by the subsidence fraction (fraction of the domain with downward vertical velocity at 500 hPa, averaged daily) is reduced relative to RCE (Table 1, Table S9 in Supporting Information S1), and the mean RH can be 10%–20% larger (Figures S1 and S2 in Supporting Information S1).

The differences in the humidity and cloud fields that result from rotation impact the flux of energy through the atmosphere and as a result, the effective feedback of the climate system. Using simple energy balance models (e.g., Becker & Wing, 2020; Cess et al., 1989), the climate feedback parameter is $\lambda = dR/dT$, and the climate sensitivity is $CS = -F/\lambda$, where dR/dT is the change with surface temperature of the net incoming radiation at the top of the atmosphere and F is a general radiative forcing, often assumed to be due to CO_2 forcing. We find that $\lambda = -1.9$ Wm^{-2} K^{-1} for the RRCE experiments with CAM6. This is less negative than in the analogous RCE

experiments ($\lambda = -2.8$ Wm^{-2} K^{-1}). If $F = 3.7$ Wm^{-2} for a doubling of CO_2 concentration, then the implied CS value is 1.9 K for CAM6 in the RRCE experiments and 1.3 K in the RCE experiments. See Supporting Information S1 for details and CAM5 values. Variations in λ are due to both shortwave λ_{SW} and longwave λ_{LW} components and are given in Table S4 of the Supporting Information S1. We calculate the cloud radiative effect (CRE = All-sky radiance − Clear-sky radiance) at the top of the atmosphere to quantify the impact that humidity and clouds have on the flux of radiant energy. Variations in λ_{SW} are due entirely to the CRE; however, variations in the λ_{LW} are due to both the CRE and changes in the clear sky radiative fluxes. The increasing CS in our RRCE experiments is due to the changes of λ_{LW}. In particular, with rotation we find less cloud radiative cooling in regions with ascent (not shown), consistent with the increased upper-level clouds and a smaller increase of mean OLR with warming (Table 1). This implies that rotation alters the distribution of water vapor enough that the response to warming of the clear-sky longwave radiation differs from the RCE case.

5. TC-Like Vortices and the Absence of Large-Scale Baroclinicity

One obvious impact of introducing rotation to a global RCE system is the presence of a vorticity field that results in cyclones throughout the domain (e.g., Bretherton et al., 2005; Chavas & Reed, 2019; Held & Zhao, 2008; Khairoutdinov & Emanuel, 2013). Unlike the random movement of organized convective regions in non-rotating systems, the meridional gradient of the planetary vorticity field creates a beta-drift that systematically drives cyclones poleward and westward (Holland, 1983). TCLVs form within 10–20 days and reach an approximately steady number within about 30–40 days (Figures S6 and S7 in Supporting Information S1). At nearly the same time the TCLVs begin to form, the V_{rms} goes through a large increase that helps to moisten and warm the troposphere, as discussed in Section 3. When rotation is added to RCE simulations, *PW* is substantially increased (Figure 3a, Table 1, Table S1 in Supporting Information S1) with negative *PW* anomalies in the tropics and positive anomalies in the higher latitudes (Figure 3b). Thus, in addition to moistening the atmosphere, another impact of rotation is the transport of moisture poleward. We hypothesize, but do not prove, that much of this poleward moisture transport is accomplished by eddies in the form of TCLVs. Figures 3c–3f provides support of this hypothesis. Tracking the moisture contained within the area defined by the TCLVs using TempestExtremes (Ullrich & Zarzycki, 2017; Ullrich et al., 2021) reveals a large poleward increase of the *PW* within the TCLVs (Figure 3c). Increased *PW* at high latitudes is not due to increased evaporation or moisture advection by a mean meridional circulation. Precipitation is greater than the evaporation poleward of about 40° latitude (Figure 3d) and the mean meridional circulation is negligible. Poleward of about 45° latitude, the zonal mean zonal wind (Figure 3f) is less than 1 m/s. The zonal mean meridional wind (not shown) is less than 1 m/s throughout the domain. We do not expect transport by eddies that are driven by baroclinic instability because our simulations have uniform SST and much of the troposphere has a barotropic structure with a meridional gradient of anomalous temperature that is 4 K or less between the equator and pole (Figure 3e) below 500 hPa. Time series of the number of TCLVs reveal a sharp increase at about the same time (2–3 weeks) that V_{rms} increases (Figures S6 and S7 in Supporting Information S1). Recall from Section 3 that this increase of V_{rms} drives an increase of both *LH* and *SH* that moistens and warms the troposphere. We suspect that the poleward movement of the TCLVs (see Movies S1–S4) transports moist convective regions through the dry midlatitude regions seen in Figure 1 and Figure S3 in Supporting Information S1, resulting in fewer regions with extremely low *RH*.

Using the CAM5 RRCE model with a grid-spacing of approximately 28 km, Stansfield and Reed (2021) found that the overall TCLV count decreased with warming but that, on average, the intensity, outer circulation size, and rates of extreme precipitation within the storms increased. Relative to the higher resolution experiments of Stansfield and Reed (2021), our TCLVs have a lower intensity (on the order of 20 m/s, relative to 35 m/s) and are larger in area and more numerous (not shown). Walsh et al. (2020) recently showed that in aquaplanet experiments increasing σ led to fewer TCs. This is consistent with our results for both CAM5 and CAM6 results (TCLV 2 years counts are 2,219, 1,954, and 1,497 for CAM6) in which the TCLV count decreases by more than 30% with a 10 K increase of SST (σ increases with SST, Figure 2e).

6. Discussion and Conclusions

The results presented here show that rotation leads to a mean climate state that is substantially different from that of non-rotating RCE. These rotating RCE simulations are a conceptually simple and relatively inexpensive configuration that increase the utility of climate models. In this regard, RRCE, along with RCE, mock-Walker,

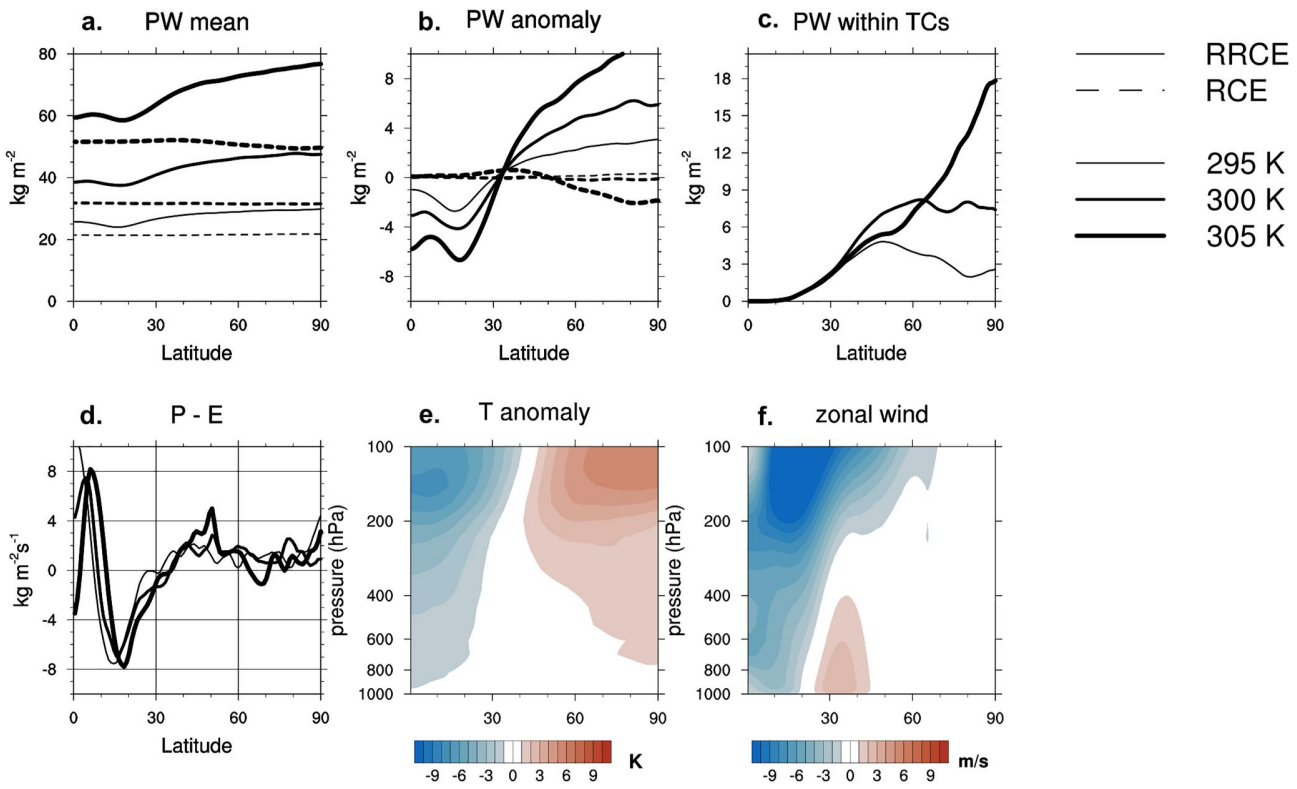

Figure 3. Zonal mean profiles of (a) climatological *PW*, (b) *PW* anomalies, (c) *PW* within cyclones, (d) zonal mean precipitation (*P*) minus evaporation (*E*), (e) zonal mean temperature anomalies relative to each vertical model level, and (f) zonal mean zonal wind. Thickness of lines increases with increasing SST. All data from CAM6. Panels (e and f) show data from the SST = 300 K RRCE simulation.

and aquaplanet simulations, occupy part of a complexity hierarchy of climate models that should be used to help guide our exploration of particular physical processes. Relative to RCE, we find that in RRCE simulations:

- Tropospheric residence time of water vapor is increased while the residence time of condensed water is slightly decreased.
- *RH* increases in the mid-troposphere.
- The intensity of the overturning circulation and the convective aggregation both decrease while *P* and *PW* increase.
- σ is larger while Q remains approximately constant resulting in a smaller diabatic velocity ($\omega_d = -Q/\sigma$).
- The effective climate sensitivity increases due to changes in the longwave feedback parameter (both clear-sky and all-sky fluxes).

Most of these changes derive from the fact that rotation increases the surface wind speed, which has a large impact on the surface flux of temperature and moisture into the atmosphere. How the atmosphere responds to this change in the surface flux, and what climate state is reached in equilibrium will likely be dependent on the details of the model configuration and parameterizations. The implication is that both the adjustment to equilibrium and the resulting climate state are important. While the obvious impact of adding rotation to simulations of RCE is the generation of TCLVs, there are numerous other characteristics of the rotating climate which play a major role in determining the hydrologic cycle and the effective climate sensitivity. The higher effective climate sensitivity is interesting because RCE simulations tend to have a lower effective climate sensitivity than do the corresponding Earth-like simulations of the parent models (e.g., Popke et al., 2013). Our study implies that one of the reasons the effective climate sensitivity of RCE experiments is low is because the troposphere is relatively dry and cooling by outgoing longwave radiation is more effective.

Both the persistently large range of projected climate sensitivity (Sherwood et al., 2020) and the dominant influence of parameterized convective schemes (Schiro et al., 2019; Tomassini et al., 2014; Zhao et al., 2016)

indicate that a deeper understanding of the Earth's climate system will require a better representation of how moisture interacts with the mean climate and the large scale circulations (Stevens & Bony, 2013). While studies of RCE have proven to be useful both for testing parameter settings of GCMs and for process level studies (e.g., Held & Zhao, 2008; Romps, 2014; Singh & O'Gorman, 2013), the large range of climate states found in RCE comparison studies (e.g., Silvers, Reed, & Wing, 2023; Wing et al., 2020) complicates the interpretation of results. We suspect that increasing the number of physical constraints in the experimental configuration, relative to RCE, will lead to more robust numerical results and increase the usefulness of idealized models for process studies. Two simple examples are the RRCE simulations presented here and mock-Walker simulations. The latter have been shown to be good analogs of the tropical overturning circulation (Lutsko & Cronin, 2018; Silvers & Robinson, 2021). The existence of TCLVs in simulations of RRCE will likely require longer simulations to achieve robust statistics relative to RCE, and the potential sensitivities of TCLVs to details in the parameterizations of the convection and micro-physics could produce a large range of results from different models. The key findings of this study are robust between the CAM5 and CAM6 models, and simulating multiple years with these models is still much less expensive computationally than RRCE simulations at convection permitting scales on smaller domains. One of our motivations is to facilitate future process studies with CAM5 and CAM6. The development of CESM2 revealed numerous interesting results (Danabasoglu et al., 2020) including an unexpected evolution of the historical global mean temperature, relatively thick clouds in the arctic, and unexpectedly high values of the ECS. Each of these characteristics could be closely tied to the parameterization of clouds and the parameter settings that were used for CESM2. RRCE simulations are conceptually simple and numerically inexpensive tools with which cloud characteristics and sensitivities of the climate system can be probed.

Data Availability Statement

All official RCEMIP CAM output is available at http://hdl.handle.net/21.14101/d4beee8e-6996-453e-bbd1-ff53b6874c0e hosted by the German Climate Computing Center (DKRZ); native CAM output is accessible through NCAR Campaign Storage via Globus. Data files and analysis scripts for the RRCE simulations are available from Silvers, Stansfield, and Reed (2023) and https://github.com/gitleviglenn/silversRRCE.

Acknowledgments
Reed and Silvers acknowledge support from NSF award numbers 1830729 and 2327958. Stansfield acknowledges support from NSF award number 2204138. We are grateful for the comments of an anonymous reviewer and a review by Timothy W. Cronin which helped to improve the manuscript. This material is based upon work supported by the National Center for Atmospheric Research, which is sponsored by the National Science Foundation under Cooperative Agreement No. 1852977. We acknowledge high-performance computing support from Cheyenne (https://doi.org/10.5065/D6RX99HX) provided by NCAR's Computational and Information Systems Laboratory, sponsored by the National Science Foundation.

References

Arnold, N. P., & Randall, D. A. (2015). Global-scale convective aggregation: Implications for the madden-Julian oscillation. *Journal of Advances in Modeling Earth Systems*, *7*(4), 1499–1518. https://doi.org/10.1002/2015MS000498

Becker, T., & Wing, A. A. (2020). Understanding the extreme spread in climate sensitivity within the radiative-convective equilibrium model intercomparison project. *Journal of Advances in Modeling Earth Systems*, *12*(10), e2020MS002165. https://doi.org/10.1029/2020MS002165

Betts, A. K. (1998). Climate-convection feedbacks: Some further issues. *Climatic Change*, *39*(1), 35–38. https://doi.org/10.1023/a:1005323805826

Bony, S., Bellon, G., Klocke, D., Sherwood, S., Fermepin, S., & Denvil, S. (2013). Robust direct effect of carbon dioxide on tropical circulation and regional precipitation. *Nature Geoscience*, *6*(6), 447–451. https://doi.org/10.1038/ngeo1799

Bony, S., Stevens, B., Coppin, D., Becker, T., Reed, K. A., Voigt, A., & Medeiros, B. (2016). Thermodynamic control of anvil cloud amount. *Proceedings of the National Academy of Sciences of the United States of America*, *113*(32), 8927–8932. https://doi.org/10.1073/pnas.1601472113

Bretherton, C. S., Blossey, P. N., & Khairoutdinov, M. (2005). An energy-balance analysis of deep convective self-aggregation above uniform SST. *Journal of the Atmospheric Sciences*, *62*(12), 4273–4292. https://doi.org/10.1175/jas3614.1

Carstens, J. D., & Wing, A. A. (2022). A spectrum of convective self-aggregation based on background rotation. *Journal of Advances in Modeling Earth Systems*, *14*(5). https://doi.org/10.1029/2021MS002860

Carstens, J. D., & Wing, A. A. (2023). Regimes of convective self-aggregation in convection-permitting beta-plan simulations. *Journal of the Atmospheric Sciences*, *80*(9), 2187–2205. https://doi.org/10.1175/JAS-D-22-0222.1

Cess, R. D., Potter, G. L., Blanchet, J., Boer, G. J., Ghan, S. J., Kiehl, J. T., et al. (1989). Interpretation of cloud-climate feedback as produced by 14 atmospheric general circulation models. *Science*, *245*(4917), 513–516. https://doi.org/10.1126/science.245.4917.513

Chavas, D. R., & Reed, K. A. (2019). Dynamical aquaplanet experiments with uniform thermal forcing: System dynamics and implications for tropical cyclone genesis and size. *Journal of the Atmospheric Sciences*, *76*(8), 2257–2274. https://doi.org/10.1175/JAS-D-19-0001.1

Cronin, T. W., & Chavas, D. R. (2019). Dry and semidry tropical cyclones. *Journal of the Atmospheric Sciences*, *76*(1), 2193–2213. https://doi.org/10.1175/JAS-D-18-0357.1

Danabasoglu, G., Lamarque, J.-F., Bacmeister, J., Bailey, D., DuVivier, A., Edwards, J., et al. (2020). The community Earth system model version 2 (CESM2). *Journal of Advances in Modeling Earth Systems*, *12*(2), e2019MS001916. https://doi.org/10.1029/2019ms001916

Hartmann, D. L., & Larson, K. (2002). An important constraint on tropical cloud-climate feedback. *Geophysical Research Letters*, *29*(20), 12-1–12-4. https://doi.org/10.1029/2002GL015835

Held, I. M., & Soden, B. J. (2006). Robust responses of the hydrological cycle to global warming. *Journal of Climate*, *19*(21), 5686–5699. https://doi.org/10.1175/JCLI3990.1

Held, I. M., & Zhao, M. (2008). Horizontally homogeneous rotating radiative-convective equilibria at GCM resolution. *Journal of the Atmospheric Sciences*, *65*(6), 2003–2013. https://doi.org/10.1175/2007JAS2604.1

Holland, G. J. (1983). Tropical cyclone motion: Environmental interaction plus a beta effect. *Journal of the Atmospheric Sciences*, *40*(2), 328–342. https://doi.org/10.1175/1520-0469(1983)040<0328:tcmeip>2.0.co;2

Khairoutdinov, M., & Emanuel, K. (2013). Rotating radiative-convective equilibrium simulated by a cloud-resolving model. *Journal of Advances in Modeling Earth Systems*, *5*(4), 816–825. https://doi.org/10.1002/2013MS000253
Kiladis, G. N., Wheeler, M. C., Haertel, P. T., Straub, K. H., & Roundy, P. E. (2009). Convectively coupled equatorial waves. *Reviews of Geophysics*, *47*(2), RG2003. https://doi.org/10.1029/2008RG000666
Kirtman, B. P., & Schneider, E. K. (2000). A spontaneously generated tropical atmospheric general circulation. *Journal of the Atmospheric Sciences*, *57*(13), 2080–2093. https://doi.org/10.1175/1520-0469(2000)057⟨2080:ASGTAG⟩2.0.CO;2
Knutson, T. R., & Manabe, S. (1995). Time-mean response over the tropical Pacific to increased CO_2 in a coupled ocean-atmosphere model. *Journal of Climate*, *8*(9), 2181–2199. https://doi.org/10.1175/1520-0442(1995)008⟨2181:TMROTT⟩2.0.CO;2
Lutsko, N. J., & Cronin, T. W. (2018). Increase in precipitation efficiency with surface warming in radiative-convective equilibrium. *Journal of Advances in Modeling Earth Systems*, *10*(11), 2992–3010. https://doi.org/10.1029/2018MS001482
Manabe, S., & Wetherald, R. T. (1967). Thermal equilibrium of the atmosphere with a given distribution of relative humidity. *Journal of the Atmospheric Sciences*, *24*(3), 241–259. https://doi.org/10.1175/1520-0469(1967)024<0241:teotaw>2.0.co;2
Merlis, T. M., Zhou, W., Held, I. M., & Zhao, M. (2016). Surface temperature dependence of tropical cyclone-permitting simulations in a spherical model with uniform thermal forcing. *Geophysical Research Letters*, *43*(6), 2859–2865. https://doi.org/10.1002/2016GL067730
Muller, C. J., & Held, I. (2012). Detailed investigation of the self-aggregation of convection in cloud-resolving simulations. *Journal of the Atmospheric Sciences*, *69*(8), 2551–2565. https://doi.org/10.1175/JAS-D-11-0257.1
O'Gorman, P. A., Allan, R. P., Byrne, M., & Previdi, M. (2012). Energetic constraints on precipitation under climate change. *Surveys in Geophysics*, *33*(3–4), 585–608. https://doi.org/10.1007/s10712-011-9159-6
Pierrehumbert, R. T. (1995). Thermostats, radiator fins, and the local runaway greenhouse. *Journal of the Atmospheric Sciences*, *52*(10), 1784–1806. https://doi.org/10.1175/1520-0469(1995)052⟨1784:TRFATL⟩2.0.CO;2
Pierrehumbert, R. T., Brogniez, H., & Roca, R. (2007). On the relative humidity of the atmosphere. In T. Schneider, & A. H. Sobel (Eds.), *The global circulation of the atmosphere* (pp. 143–185). Princeton University Press.
Popke, D., Stevens, B., & Voigt, A. (2013). Climate and climate change in a radiative-convective equilibrium version of ECHAM6. *Journal of Advances in Modeling Earth Systems*, *5*, 1–14. https://doi.org/10.1029/2012MS000191
Reed, K. A., & Chavas, D. R. (2015). Uniformly rotating global radiative-convective equilibrium in the community atmosphere model, version 5. *Journal of Advances in Modeling Earth Systems*, *7*(4), 1938–1955. https://doi.org/10.1002/2015MS000519
Reed, K. A., Medeiros, B., Bacmeister, J. T., & Lauritzen, P. H. (2015). Global radiative–convective equilibrium in the community atmosphere model, version 5. *Journal of the Atmospheric Sciences*, *72*(5), 2183–2197. https://doi.org/10.1175/jas-d-14-0268.1
Reed, K. A., Silvers, L. G., Wing, A. A., Hu, I.-K., & Medeiros, B. (2021). Using radiative convective equilibrium to explore clouds and climate in the community atmosphere model. *Journal of Advances in Modeling Earth Systems*, *13*(12). https://doi.org/10.1029/2021MS002539
Romps, D. M. (2014). An analytical model for tropical relative humidity. *Journal of Climate*, *27*(19), 7432–7449. https://doi.org/10.1175/jcli-d-14-00255.1
Schiro, K. A., Su, H., Wang, Y., Langenbrunner, B., Jiang, J. H., & Neelin, J. D. (2019). Relationships between tropical ascent and high cloud fraction changes with warming revealed by perturbation physics experiments in CAM5. *Geophysical Research Letters*, *46*(16), 10112–10121. https://doi.org/10.1029/2019GL083026
Sherwood, S. C., Webb, M. J., Annan, J. D., Armour, K. C., Forster, P. M., Hargreaves, J. C., et al. (2020). An assessment of Earth's climate sensitivity using multiple lines of evidence. *Reviews of Geophysics*, *58*(4), e2019RG000678. https://doi.org/10.1029/2019RG000678
Shi, X., & Bretherton, C. S. (2014). Large-scale character of an atmosphere in rotating radiative-convective equilibrium. *Journal of Advances in Modeling Earth Systems*, *6*(3), 616–629. https://doi.org/10.1002/2014MS000342
Silvers, L. G., Reed, K. A., & Wing, A. A. (2023). The response of the large-scale tropical circulation to warming. *Journal of Advances in Modeling Earth Systems*, *15*(3). https://doi.org/10.1029/2021MS002966
Silvers, L. G., & Robinson, T. (2021). Clouds and radiation in a mock-walker circulation. *Journal of Advances in Modeling Earth Systems*, *13*(2). https://doi.org/10.1029/2020MS002196
Silvers, L. G., Stansfield, A., & Reed, K. A. (2023). The impact of rotation on tropical climate, the hydrologic cycle, and climate sensitivity [Dataset]. Dryad. https://doi.org/10.5061/dryad.qfttdz0q1
Singh, M. S., & O'Gorman, P. A. (2013). Influence of entrainment on the thermal stratification in simulations of radiative-convective equilibrium. *Geophysical Research Letters*, *40*(16), 4398–4403. https://doi.org/10.1002/grl.50796
Stansfield, A. M., & Reed, K. A. (2021). Tropical cyclone precipitation response to surface warming in aquaplanet simulations with uniform thermal forcing. *Journal of Geophysical Research: Atmospheres*, *126*(24), e2021JD035197. https://doi.org/10.1029/2021JD035197
Stevens, B., & Bony, S. (2013). What are climate models missing? *Science*, *340*(6136), 1053–1054. https://doi.org/10.1126/science.1237554
Tobin, I., Bony, S., & Roca, R. (2012). Observational evidence for relationships between the degree of aggregation of deep convection, water vapor, surface fluxes, and radiation. *Journal of Climate*, *25*(20), 6885–6904. https://doi.org/10.1175/jcli-d-11-00258.1
Tomassini, L., Voigt, A., & Stevens, B. (2014). On the connection between tropical circulation, convective mixing, and climate sensitivity. *Quarterly Journal of the Royal Meteorological Society*, *141*(689), 1404–1416. https://doi.org/10.1002/qj.2450
Ullrich, P. A., & Zarzycki, C. M. (2017). TempestExtremes: A framework for scale-insensitive pointwise feature tracking on unstructured grids. *Geoscientific Model Development*, *10*(3), 1069–1090. https://doi.org/10.5194/gmd-10-1069-2017
Ullrich, P. A., Zarzycki, C. M., McClenney, E. E., Pinheiro, M. C., Stansfield, A. M., & Reed, K. A. (2021). Tempest extremes v2.0: A community framework for feature detection, tracking and analysis in large datasets. *Geoscientific Model Development*, *14*(8), 5023–5048. https://doi.org/10.5194/gmd-14-5023-2021
Walsh, K., Sharmila, S., Thatcher, M., Wales, S., Utembe, S., & Vaughan, A. (2020). Real world and tropical cyclone world. Part II: Sensitivity of tropical cyclone formation to uniform and meridionally varying sea surface temperatures under aquaplanet conditions. *Journal of Climate*, *33*(4), 1473–1486. https://doi.org/10.1175/JCLI-D-19-0079.1
Webster, P. J. (1994). The role of hydrological processes in ocean-atmosphere interactions. *Reviews of Geophysics*, *32*(4), 427–476. https://doi.org/10.1029/94RG01873
Wing, A. A., Camargo, S. J., & Sobel, A. H. (2016). Role of radiative-convective feedbacks in spontaneous tropical cyclogenesis in idealized numerical simulations. *Journal of the Atmospheric Sciences*, *73*(7), 2633–2642. https://doi.org/10.1175/JAS-D-15-0380.1
Wing, A. A., & Emanuel, K. A. (2014). Physical mechanisms controlling self-aggregation of convection in idealized numerical modeling simulations. *Journal of Advances in Modeling Earth Systems*, *6*(1), 59–74. https://doi.org/10.1002/2013MS000269
Wing, A. A., Emanuel, K. A., Holloway, C. E., & Muller, C. (2017). Convective self-aggregation in numerical simulations: A review. *Surveys in Geophysics*, *11*(38), 1173–1197. https://doi.org/10.1007/s10712-017-9408-4
Wing, A. A., Reed, K. A., Satoh, M., Stevens, B., Bony, S., & Ohno, T. (2018). Radiative–convective equilibrium model intercomparison project. *Geoscientific Model Development*, *11*(2), 793–813. https://doi.org/10.5194/gmd-11-793-2018

Wing, A. A., Stauffer, C. L., Becker, T., Reed, K. A., Ahn, M.-S., Arnold, N. P., et al. (2020). Clouds and convective self-aggregation in a multi-model ensemble of radiative-convective equilibrium simulations. *Journal of Advances in Modeling Earth Systems*, *12*(9), e2020MS002138. https://doi.org/10.1029/2020MS002138

Zelinka, M. D., & Hartmann, D. L. (2010). Why is longwave cloud feedback positive? *Journal of Geophysical Research*, *115*(D16), D16117. https://doi.org/10.1029/2010JD013817

Zhao, M., Golaz, J.-C., Held, I. M., Ramaswamy, V., Lin, S.-J., Ming, Y., et al. (2016). Uncertainty in model climate sensitivity traced to representations of cumulus precipitation microphysics. *Journal of Climate*, *29*(2), 543–560. https://doi.org/10.1175/JCLI-D-15-0191.1